Effect of Composition and Processing Conditions on the Chemical and Morphological Evolution of PA-6/EPM/EPM-*g*-MA Blends in a Corotating Twin-Screw Extruder

A. V. MACHADO,[1] J. A. COVAS,[1] M. WALET,[2] M. VAN DUIN[2]

[1] Department of Polymer Engineering, University of Minho, 4800 Guimarães, Portugal

[2] DSM Research, P.O. Box 18, 6160 MD, Geleen, The Netherlands

Received 19 January 2000; accepted 19 July 2000

ABSTRACT: This study investigated the effect of blend composition and processing conditions on the chemical conversion and morphological evolution of PA-6/EPM/EPM-*g*-MA blends along a twin-screw extruder. The maleic anhydride (MA) content of the modified rubber was found to decrease strongly, to a level of almost zero, and in the melting zone the particle size was dramatically reduced, from millimeters to submicrometers. Blend composition had a secondary effect on both chemical conversion and morphological development. The processing conditions, particularly the temperature profile and the screw speed, affected both the chemical conversion and the morphological evolution. Using low temperatures and low screw rotation it was possible to follow in detail the evolution of morphological development of a reactive blend in a twin-screw extruder. © 2001 John Wiley & Sons, Inc. J Appl Polym Sci 80: 1535–1546, 2001

Key words: reactive blend; morphology; chemical conversion; polyamide-6

INTRODUCTION

Polyamides are very attractive polymers for various engineering applications, but they have some drawbacks, such as moisture uptake and low temperature toughness. In order to improve their performance, polyamides (PAs) have been blended with various rubbers,[1–5] such as acrylonitrile–butadiene–styrene (ABS), ethylene propylene (EPM), styrene–butadiene–styrene (SBS), and styrene–ethylene–butadiene–styrene (SEBS), for increased (low temperature) toughness, and with polypropylene (PP)[3–6] and polyethylene (PE)[1,7–12] in order to improve water uptake and reduce material costs. These blends are usually compatibilized via reactive blending in the presence of polymers containing maleic anhydride (MA). The MA groups of the compatibilizer react with the amine groups of the polyamide to form copolymers. It is now well accepted that these graft copolymers formed at the interface do the following: (1) lower interfacial tension, improve interfacial adhesion, and prevent coalescence, and thus they (2) decrease the domain size of the dispersed phase and stabilize the blend morphology and, consequently, they (3) determine the mechanical properties of the final blend.[1–12] Up to now most *in situ* compatibilization studies have used black-box approaches, in which blend composition, extruder layout, and processing conditions are correlated with the morphology and mechanical properties of the extruded blends. In a limited number of studies an attempt was made to gain more insight into reactive blending by drawing screws or tak-

Correspondence to: J. A. Covas.

Journal of Applied Polymer Science, Vol. 80, 1535–1546 (2001)

ing samples from the melt, followed by off-line analysis.[6,13–15] For example, it was shown[6] that the morphological development of a PP-*g*-MA/PA-6 blend is very rapid and takes place during melting. However, most such studies suffered from a sampling that was too slow, and therefore the results may not be representative. Recently, we developed a device that makes it possible within a few seconds to take representative samples of the material being processed.[16]

A series of such sampling devices was used to study the chemical conversion and the morphological evolution of reactive blends of PA-6 and EPM (PA-6/EPM and PA-6/EPM/EPM-*g*-MA) along a corotating intermeshing twin-screw extruder.[17] The MA content of the modified rubber was found to decrease strongly on the melting of the PA pellets and the melt flow through the first set of staggering kneading blocks; that is, the grafting reaction is very fast. Simultaneously, the morphology changed dramatically in this zone of the extruder, from a millimeter to a submicrometer level. Farther downstream the chemical conversion and the morphology hardly changed anymore.

It would be interesting to study the effect of several variables on the chemical reaction and the morphological evolution along the extruder in order to obtain more detailed information about the physicochemical processes occurring during blending, such as the eventual development of occlusions of PA-6 on the dispersed rubber particles. In the present study several routes were followed in order to reach these goals. MA-containing materials with softening/melting temperatures higher than EPM (T_g = −45°C) were used: PE-*g*-MA (T_m = 132°C), PP-*g*-MA (T_m = 165°C), and SMI (T_g = 190°C). PA-6/EPM-*g*-MA blends with varying compositions based on changing the ratio of anhydride to amine groups were prepared. The feeding sequence of the blend components and the processing conditions (screw speed and temperature profile) were also varied.

EXPERIMENTAL

Materials

PA-6 (Akulon® K123 with M_n = 13.00 g/mol, NH_2 = 55 meq/g, and COOH = 60 meq/g), PE-*g*-MA (HDPE, 0.93 wt % MA) and SMA imidized with aniline (SMI, 1.4 wt % MA) were obtained from DSM, the Netherlands. EPM-*g*-MA (Exxelor VA 1801: 0.49 wt % MA) and PP-*g*-MA (Epolene E-43 and G-3003, with 2.5 and 0.3 wt % MA, respectively) were kindly supplied by Exxon (Barcelona, Spain) and Eastman Kodak, (Kingsport, TN), respectively.

The composition of the various blends studied in this work is shown in Table I. Using blend 1 as the basis for comparison, in blends 2–5 the EPM-*g*-MA was replaced, respectively, by PE-*g*-MA, PP-*g*-MA, and SMI. In blends 6–8 the PA/EPM blend ratio was changed; that is, the ratio of reactive groups (amine and MA) was varied from 2.2 to 0.06 mol NH_2/mol MA. In blend 9 EPM with hydrolyzed MA groups (24 h in boiling water) was used. Blends 10–13 had the same PA/EPM-*g*-MA composition but were prepared using different processing conditions.

Blend Preparation

All experiments were carried out in a laboratory modular Leistritz LSM 30.34 intermeshing corotating twin-screw extruder. As illustrated in Figure 1, two screw configurations were used in this study [Fig. 1(a,b), respectively]. In order to collect small amounts of sample from the extruder during blending, sampling devices were inserted at specific locations (denoted by capital letters in the figures) along the barrel, as detailed by Machado.[17] The locations selected generally were zones where high pressure was developed because these were not only the sites of the main changes in morphology and chemistry but also because these locations are where polymer melt can more easily be removed from the barrel. Around 2 g of a sample was collected within 2–3 s. In order to avoid additional reaction and/or morphological changes such as coalescence of the dispersed phase, all samples were quenched in liquid nitrogen for subsequent characterization.

Blends 1 to 9 were compounded under identical processing conditions (Table I) using the screw configuration shown in Figure 1(a), which included three mixing zones comprising staggered kneading blocks so that significant dispersive mixing downstream was produced. The first kneading block was followed by a reverse element, thus inducing complete melting, while the final mixing section contributed to an effective venting.

For blend 10 the two polymers were fed separately. PA-6 was starve-fed as usual, and after melting, EPM-*g*-MA was added downstream. The screw configuration, as well as the feeding and

Table I Composition and Processing Conditions of Blends of PA-6 and MA-Containing Polymers

(Set Temperature = 230°C; Throughput = 6 kg/h; Screw Rotation = 200 rpm)

Blend	PA-6 (wt %)	MA-Containing Polymer (wt %)	Extruder Layout (Figure 1)	Comments
1	80	EPM-*g*-MA (20)	a	
2	80	PE-*g*-MA (20)	a	0.93 wt % MA
3	80	PP-*g*-MA1 (20)	a	2.5 wt % MA
4	80	PP-*g*-MA2 (20)	a	0.3 wt % MA
5	80	SMI (20)	a	1.4 wt % MA
6	50	EPM-*g*-MA (50)	a	
7	20	EPM-*g*-MA (80)	a	
8	10	EPM-*g*-MA (90)	a	
9	80	EPM-*g*-MA (20)	a	hydrolyzed MA groups
10	80	EPM-*g*-MA (20)	b	side feed of EPM-*g*-MA
11	80	EPM-*g*-MA (20)	c	
12	80	EPM-*g*-MA (20)	c	Low set temperature profile in first part of extruder
13	80	EPM-*g*-MA (20)	c	screw rotation = 120 rpm throughput = 4 kg/h low set temperature in first part of extruder

sampling locations, are indicated in Figure 1(b). The screw setup for this experiment included a first kneading section with neutral staggering disks and a left-ended element in order to ensure complete PA melting; a conveying zone for rubber feeding; as well as a second kneading section with neutral staggering elements to promote chemical reaction and development of morphology. A third mixing section before vacuum ensured further mixing. Blends 11–13 were prepared using the extruder layout depicted in Figure 1(c). The screw configuration is the same as that in Figure 1(a), but the barrel setup provided for collecting more samples along the screw. Devolatilization before pumping the melt through the die was common to all experiments.

Materials Characterization

Since in a previous study[17] good agreement between FTIR and the nitrogen content data had been obtained, that is, between the residual MA content and the amount of graft PA, in this study only FTIR data was used for chemical characterization. The samples collected along the extruder were analyzed following the methodology previously developed[4] and illustrated in Figure 2. Milled samples were hydrolyzed with refluxing 6*N* hydrochloric acid during 6 h. Thin films of the residues were prepared by compression molding and were analyzed by FTIR (PerkinElmer 1720 spectrometer). The residual MA content was quantified using the anhydride carbonyl absorption at 1785 cm^{-1} after IR calibration with a set of references. The MA conversion (in percent) is defined as $[(MA_{original} - MA_{residual})/MA_{original}] \times 100$.

The morphology of the blends was analyzed by electron microscopy using a Philips CM200 transmission electron microscope (TEM). For this purpose, very thin coupes (70 nm) were cut at −100°C from samples previously stained with a 50:50 osmium tetroxide:formaldehyde mixture. Some samples were characterized using a Jeol JSM 6310F scanning electron microscope (SEM) after extraction of the rubber with boiling xylene. The average size and the size distribution of the dispersed phase were determined from TEM and SEM micrographs using an automatic method of image analysis (Leica Quantimet 550), assuming an equivalent circle diameter for each particle, explained in detail by Machado et al.[17] To obtain results, typically 200 particles were studied.

RESULTS AND DISCUSSION

Change of MA-Containing Polymers

The residual MA contents of the MA-containing polymers of the PA-6 blends sampled along the extruder, as determined by FTIR, are given in Table II. As shown in a previous study,[17] the MA content of the EPM-*g*-MA in a PA-6/EPM-*g*-MA

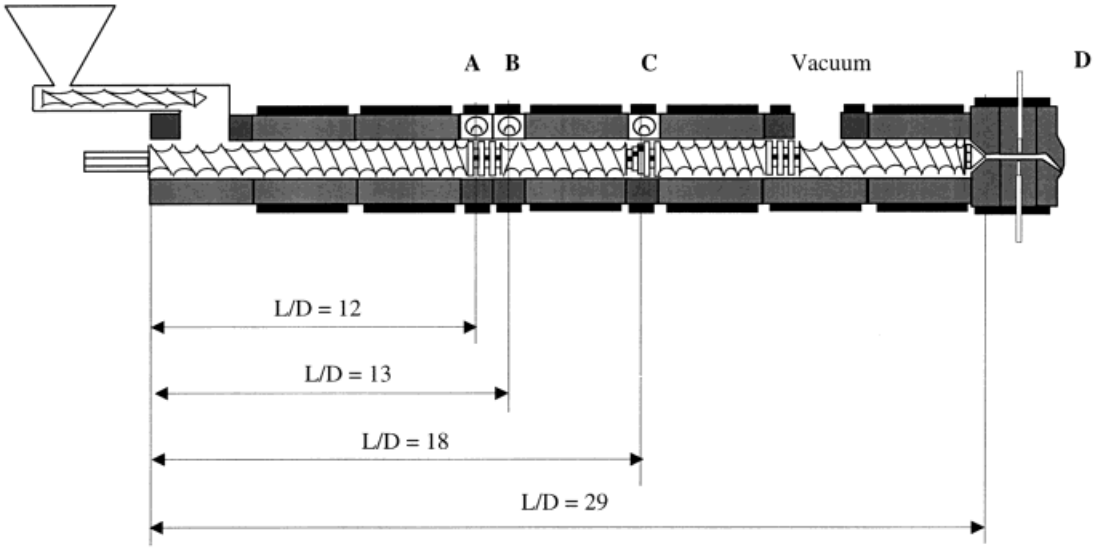
A
B
C
Vacuum
D
L/D = 12
L/D = 13
L/D = 18
L/D = 29

(a)

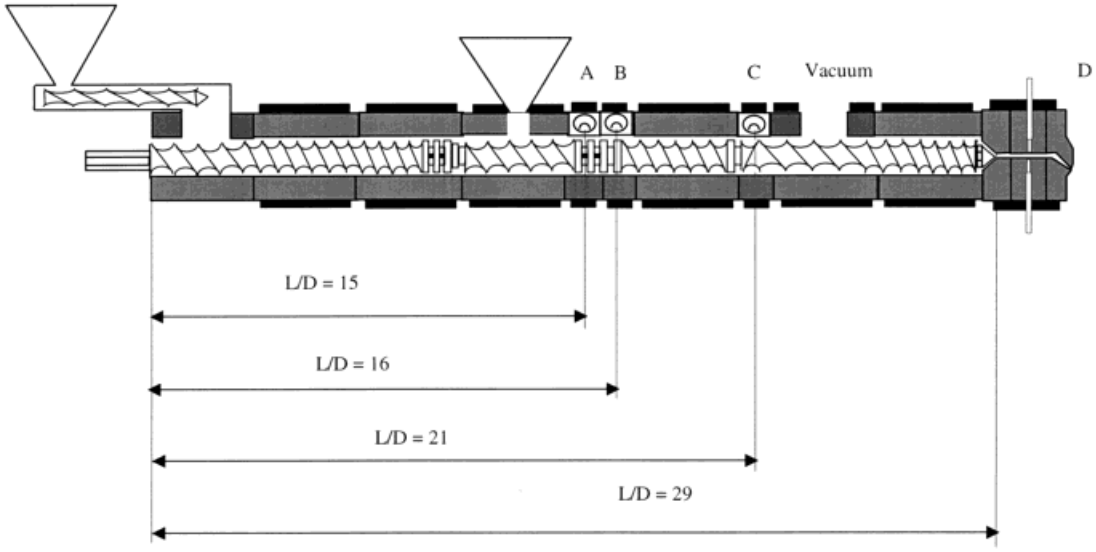
A
B
C
Vacuum
D
L/D = 15
L/D = 16
L/D = 21
L/D = 29

(b)

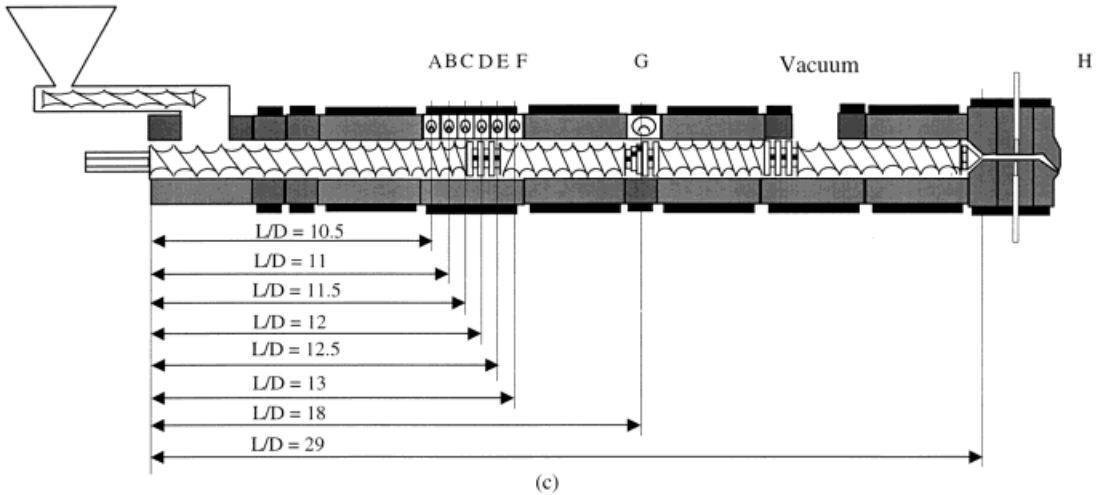
ABCDEF
G
Vacuum
H
L/D = 10.5
L/D = 11
L/D = 11.5
L/D = 12
L/D = 12.5
L/D = 13
L/D = 18
L/D = 29

(c)

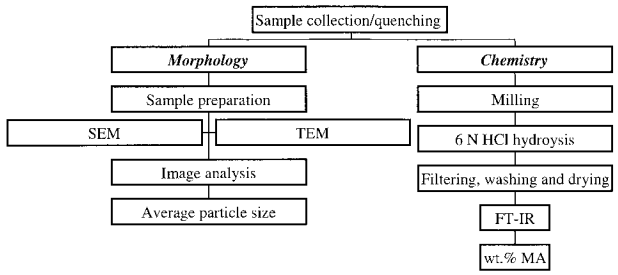

Figure 2 Characterization of collected PA-6 blend samples.

(80/20 w/w) blend (blend 1) decreased strongly from 0.7 to less than 0.1 wt % at sampling position A, that is, on melting. When, instead of EPM-*g*-MA, MA-containing polymers with a higher softening/melting temperature—PE-*g*-MA, PP-*g*-MA, and SMI (blends 2 to 5)—were used as the minor blend phase, the results were significantly different. As shown in Figure 3, the residual MA contents were relatively high at location A, decreased up to location C, and then remained fairly constant. The results show that when the softening/melting temperature of the MA-containing polymer increases [EPM-*g*-MA → PE-*g*-MA → PP-*g*-MA(1 and 2) → SMI] melting and subsequent blend dispersion is delayed, resulting in a slower MA conversion. In the case of PE-*g*-MA and PP-*g*-MA2, the physicochemical processes are still fast enough to produce more or less full MA conversion. For PP-*g*-MA1, the original MA content is probably too high to reach complete MA conversion even at the die. Nevertheless, the absolute MA conversion of PP-*g*-MA1 is relatively large (2.5 → 1.4 wt % MA), again indicating that *in situ* compatibilization is a very fast process. Finally, for the MA-containing polymer with the highest softening point, that is, SMI, the reactive blending process is slowed down considerably, as shown by the small absolute and relative MA conversions (1.4 → 1.1 wt % MA and 20%, respectively).

The morphological evolution of a selected number of blends was determined. Table II presents the evolution of particle size and particle size distribution along the extruder in terms of average size, range of sizes, and variance. Although the MA conversion of the PA-6/PP-*g*-MA1 blend (blend 3) was clearly far from complete, the dispersion of this blend is more or less accomplished at location A (Fig. 4), where the average particle size is approximately 0.5 μm. Only a decrease in the particle size distribution can be seen thereafter, as observed with blend 1. This is consistent with the high absolute MA conversion (Table II). The subsequent increase of MA conversion beyond location A hardly affects the morphology of the PA-6/PP-*g*-MA blend. Hence, the differences in particle size of the PA-6 blends with varying MA-containing polymers (blends 2 to 5) collected at the die are probably not a result of differences in the conversion of the reactive blending process but are most likely related to differences in viscosity and interfacial tension.

Change of PA-6/EPM-*g*-MA Blend Composition

The composition of the PA-6/EPM-*g*-MA blends was varied in order to have different ratios of reactive groups (MA and amine) and to study their effect on chemistry and blend morphology. The results presented in Table II and Figure 5 for blends 1 and blends 6–8 show a substantial decrease in the MA content at the first kneading zone (location A), from 0.5 to approximately 0.1 wt % MA and only a slight decrease farther downstream. In all cases, the *in situ* compatibilization reactions occurred in the melting zone within a few seconds, regardless of the ratio of the MA and amine groups in the blend. Nevertheless, the interfacial structure in these blends is distinct because the average length of the PA grafts decreases as the composition of the PA-6/EPM-*g*-MA blends goes from 80/20 to 10/90. In the former, the original MA/amine molar ratio is 0.13, and PA chains are predominantly coupled to EPM-*g*-MA chains via the PA amine end groups. In the latter (10/90 w/w) the MA/amine ratio is 4.5, and the MA conversion is still more or less complete. Therefore, not only the PA amine end groups but also the PA chain amide groups must have reacted with the EPM-*g*-MA. As a result, PA chain scission must have occurred, resulting in relatively short lengths of the PA grafts.[14]

The morphological development of blends 6 and 7 along the extruder was not studied because it must be similar to that of blend 1, with relative differences directly explainable by differences in

Figure 1 Screw configurations and sampling locations used in this study: (a) blends 1–9, (b) blend 10, and (c) blends 11–13.

Table II Chemical Conversion, Particle Size, and Particle Size Distribution of Blends of PA-6 with MA-Containing Polymers as Function of Screw Length

Blend	Sampling Location	Residual MA Content of MA-Containing Polymer (wt %)	Reacted MA (%)	Particle Size		
				Average (μm)	Range (μm)	Variance (μm^2)
1	A	0.07	86	0.48	0.16–1.38	0.06
	B	0.07	86	0.35	0.15–0.74	0.03
	C	0.08	84	0.33	0.16–0.75	0.02
	D	0.07	86	—	—	—
2	A	0.30	68	—	—	—
	B	0.21	77	—	—	—
	C	0.16	82	—	—	—
	D	0.13	85	0.22	0.13–0.54	0.02
3	A	1.89	25	0.46	0.17–3.92	0.36
	B	1.58	37	0.42	0.15–2.91	0.22
	C	1.52	40	0.44	0.15–2.51	0.22
	D	1.48	42	0.44	0.15–2.90	0.26
4	A	0.08	72	—	—	—
	B	0.07	77	—	—	—
	C	0.04	87	—	—	—
	D	0.04	87	—	—	—
5	A	1.34	5	—	—	—
	B	1.20	14	—	—	—
	C	1.13	20	—	—	—
	D	—	—	0.20	0.10–0.51	0.02
6	A	0.10	80	—	—	—
	B	0.07	86	—	—	—
	C	0.05	90	—	—	—
	D	—	—	—	—	—
7	A	0.10	80	—	—	—
	B	0.05	90	—	—	—
	C	0.04	92	—	—	—
	D	—	—	—	—	—
8	A	0.09	82	0.063	0.012–0.19	0.001
	B	0.07	86	0.069	0.012–0.19	0.001
	C	0.05	90	0.064	0.012–0.18	0.001
	D	0.03	94	0.060	0.012–0.15	0.001
9	A	0.07	86	—	—	—
	B	0.08	84	—	—	—
	C	0.06	88	—	—	—
	D	—	—	—	—	—
10	A	0.13	73	0.34	0.17–0.68	0.014
	B	0.07	86	0.31	0.15–0.56	0.010
	C	0.06	88	0.27	0.15–0.44	0.006
	D	—	—	—	—	—
11	A	0.49	0	—	—	—
	B	0.49	0	—	—	—
	C	0.13	68	—	—	—
	D	0.11	73	0.42	0.14–0.83	0.06
	E	0.07	83	—	—	—
	F	0.08	80	—	—	—
	G	—	—	—	—	—
	H	—	—	0.31	0.15–0.71	0.02

Table II *Continued*

Blend	Sampling Location	Residual MA Content of MA-Containing Polymer (wt %)	Reacted MA (%)	Particle Size		
				Average (μm)	Range (μm)	Variance (μm^2)
12	A	0.49	0	—	—	—
	B	0.49	0	—	—	—
	C	0.25	49	—	—	—
	D	0.07	76	0.44	0.14–2.32	0.08
	E	0.03	86	—	—	—
	F	—	—	—	—	—
	G	—	—	—	—	—
	H	—	—	0.30	0.14–0.81	0.02
13	A	0.49	0	—	—	—
	B	0.35	29	—	—	—
	C	0.09	82	0.45	0.15–1.45	0.05
	D	0.01	98	0.30	0.14–0.62	0.02
	E	—	—	0.31	0.14–0.54	0.02
	F	—	—	—	—	—
	G	—	—	—	—	—
	H	—	—	—	—	—

blend composition. For instance, in the case of blend 8, the modified rubber is the matrix and PA-6 is the dispersed phase, as expected for a PA-6/EPM-*g*-MA volume ratio much smaller than unity. Not surprisingly, Table II shows that the average dispersed particle size and the particle size distribution are almost constant along the extruder.

Since it was not possible to slow down the *in situ* compatibilization by varying the PA-6/EPM-*g*-MA blend composition, an attempt was made to decrease the reactivity of EPM-*g*-MA by using EPM-*g*-MA hydrolyzed to its diacid form (blend 9). As shown in Table II, the residual MA content is rather low at location A and then remains constant. These results are identical to those obtained for blend 1 with nonhydrolyzed MA groups, indicating that hydrolysis of EPM-*g*-MA does not influence the formation of a PA-6/EPM-*g*-MA graft copolymer. On blending, all diacid is converted into MA and directly into imide because of grafting of the PA-6. The hydrolyzed groups are probably easily converted back to anhydrides at these elevated temperatures.

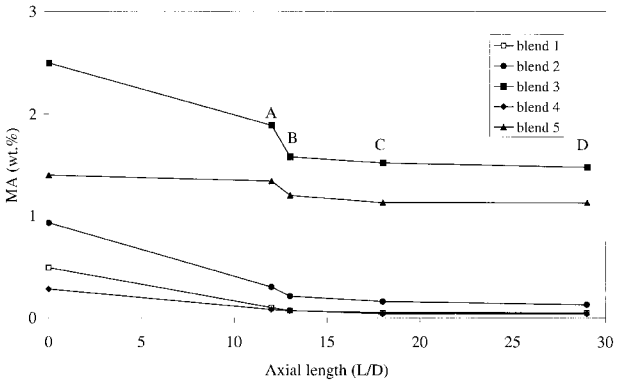

Figure 3 MA conversion of blends 1–5 along the screw for various MA-containing polymers (80/20 w/w).

Separate Feed of EPM-*g*-MA

The effect of the side feed of EPM-*g*-MA was studied for an 80/20 (w/w) composition (blend 10). Although fast chemical conversion was again observed, the residual MA content of EPM-*g*-MA at location A is significantly higher than that of the same blend prepared with premixed components (Table II, blend 10 versus blend 1, i.e., 0.13 versus 0.07 wt % MA). Here the residual MA content decreases from location A to B and then remains constant. Differences in the morphological evolution can also be observed. As shown in Figure 6(a), when using a separate feed, rubber phase dispersion is not yet complete at location A, where rubber particles with different sizes are visible. At location

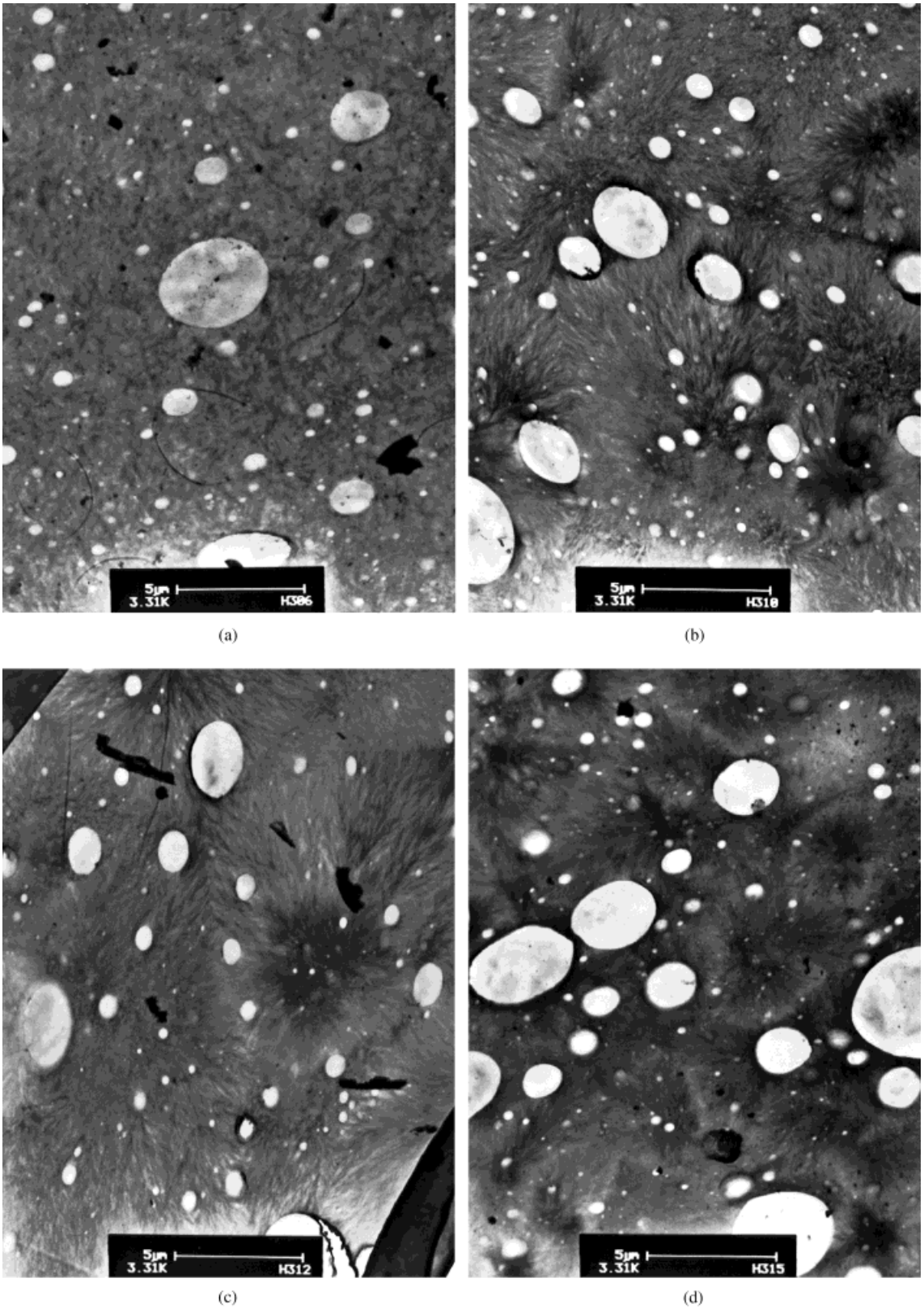

Figure 4 TEM micrographs of blend 4 [PA-6/PP-*g*-MA (80/20 w/w)] collected along the screw at locations A, B, C, and D (a, b, c, and d, respectively).

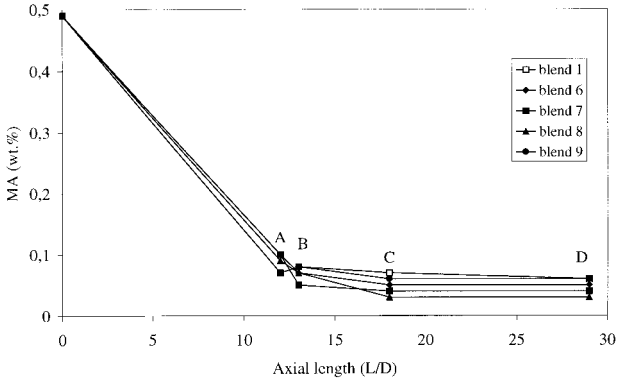

Figure 5 MA conversion of blends 1 and 6–9 [PA-6/EPM-*g*-MA] along the screw for various compositions.

B the degree of dispersion has improved, and at location C a good dispersion is obtained [Fig. 6(b)]. Table II presents a progressive decrease in both the average particle size and the particle size distribution.

Change of Processing Conditions

Given the high rate of MA conversion observed above, a special barrel segment containing six collecting devices more than 12 cm in the axis direction was designed and built. As shown in Figure 1(c), these devices replaced the previous A and B devices, thus providing more sampling for chemical and morphological characterization. Blends 11–13 were processed using this arrangement. Blends 11 and 12, which were prepared using a different temperature profile, up to *L/D* = 13, clearly yielded different results (Table II and Fig. 7). Although blend 11 exhibits roughly the same chemical evolution as blend 1, blend 12 (processed under a lower set temperature), presents a high residual MA content (0.25 wt %) at location C. In fact, PA-6 pellets embedded in a continuous rubber phase [Fig. 8(a)] can still be observed. Between locations C and D, which are only 2 cm apart in the axial direction, the material melts completely, and the MA content decreases significantly (from 0.25 to 0.09 wt %).

Since it is well known that screw speed has a strong effect on morphological development, an attempt at slowing down the *in situ* compatibilization by decreasing the screw rotation was carried out

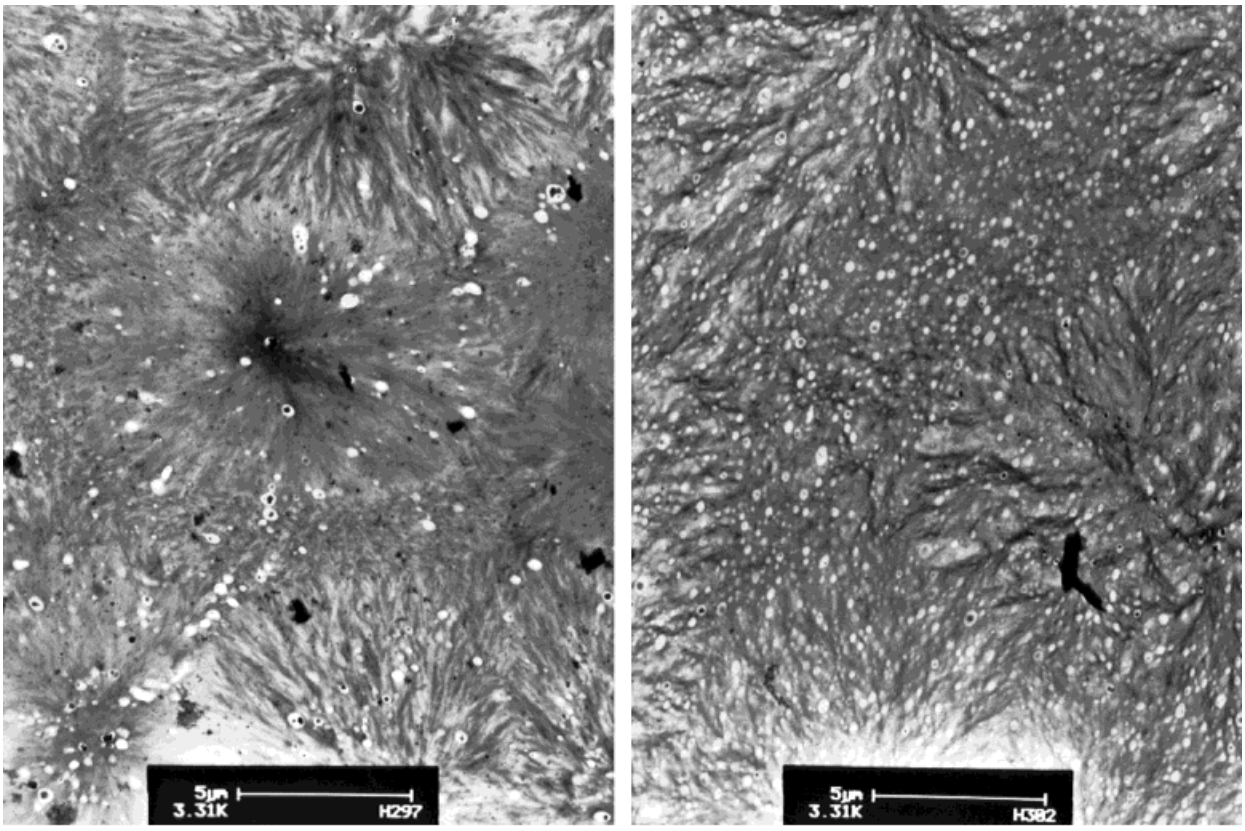

Figure 6 TEM micrographs of blend 10 [PA-6/EPM-*g*-MA (80/20 w/w)] with EPM-*g*-MA side feed sampled along the screw at locations A and C (a and b, respectively).

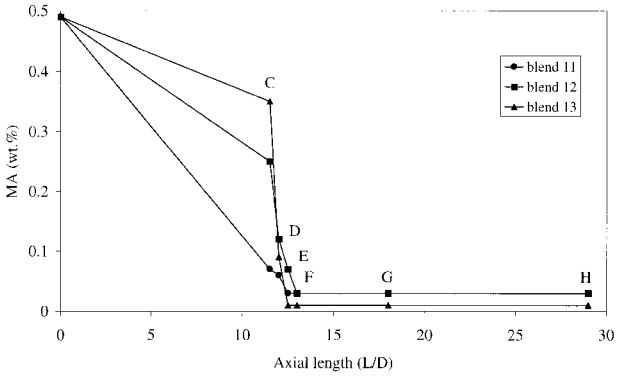

Figure 7 MA conversion of blends 11, 12, and 13 [PA-6/EPM-*g*-MA (80/20 w/w)] along the screw.

(blend 13). Although at location C the MA content is higher than for blend 12 (0.35 versus 0.25 wt %), no significant differences in morphology were observed (Table II). It is probable that more information on morphological development would be obtained when using very low screw speeds, but this would also require changes in the throughput and would be unrealistic from an industrial point of view.

Blend 12 seemed appropriate for a more detailed morphology study. SEM micrographs of this blend at location C [Fig. 8(a)] show that the rubber is molten and surrounds the PA-6 pellets. It is also possible to observe molten PA-6 threads dispersed in the rubber. These features are more clearly visible when PA-6 has been removed with formic acid [Fig. 8(b)]. TEM analysis at location C shows a very heterogeneous morphology [Fig. 8(c)]. Clearly, the dispersion process at this stage of the process is very complex. Large rubber particles and unmolten PA-6 pellets (not visible in the micrographs because they were lost during preparation of the TEM coupes) are present in close vicinity to a finely dispersed PA-6/EPM-*g*-MA mixture (rubber particle size: 0.25–1 μm). All sorts of morphologies with intermediate dimensions can be observed, including thin PA-6 regions drawn from the unmolten PA-6 pellets, EPM-*g*-MA sheets, thin elongated EPM-*g*-MA and PA-6 domains, and EPM threads in the process of breaking up. A higher magnification makes visible a very unusual morphology at the PA-6/EPM-*g*-MA interface [Fig. 8(d)]: stretched, wavelike rubber domains perpendicular to the PA-6 surface and thin spider-web-like filaments. Although most of these morphological features have been observed before for blends produced in a batch kneader,[18–19] our results were obtained in a commercial twin-screw extruder under industrially relevant processing conditions.

Finally, it is relevant to remark on the phenomenon of phase inversion, which generally has been shown to occur in A/B blends, with A the major blend component (with a higher softening point) and B the minor blend component (with a lower softening point).[18] First, B will soften and form the matrix for the not-yet-molten A phase. Then the melting of the A phase inversion occurs, yielding a blend in which A is the matrix and B the dispersed phase. However, during the experiment with the PA-6/EPM-*g*-MA (80/20 w/w) blend 12 (A/B), phase inversion was not observed. At location B—just upstream of the kneading zone—the EPM-*g*-MA crumbs are only partially stretched and glued to the PA pellets, coating partially the surface of the PA pellets. A dispersion of PA pellets in the EPM matrix is not observed, probably because of the low EPM content (20 wt %) in combination with the highly viscous character of the EPM phase. A detailed inspection of the TEM micrographs of samples taken at position C [Fig. 8(c)] indicates that the EPM phase is not continuous anywhere in the first part of the kneading/melting zone. So, for obtaining the final morphology at position D, that is, EPM particles dispersed in a continuous PA matrix, phase inversion does not occur.

Occlusions

In the blends of PA-6 with EPM-*g*-MA as the minor phase (blends 1 and 10–13) PA occlusions can be observed in the rubber particles [Fig. 8(d)]. As pointed out several others,[17–19] these occlusions may be formed on the melting of the PA-6 pellets. The PA-6 already bound at the interface is drawn into the rubber phase when the latter becomes the dispersed phase. The rubber particles themselves are then stabilized by the newly formed PA-6/EPM graft copolymer.

The fraction of rubber particles with PA occlusions was taken as a measure of the degree of occlusion. The data shown in Table III seem to indicate that the degree of occlusion does not vary along the extruder axis. Thus, as with the PA-6/EPM-*g*-MA graft copolymer formation and blend dispersion, the occlusions develop in the melting zone, that is, just before and/or in the first kneading zone, where interfacial area and high shearing are generated. The degree of occlusion of blends 1, 11, and 12 is very similar, but that of blend 10 is much smaller. In fact, when EPM-*g*-MA is side-fed after all PA-6 has become molten, most PA-6/EPM-*g*-MA graft copolymer is at

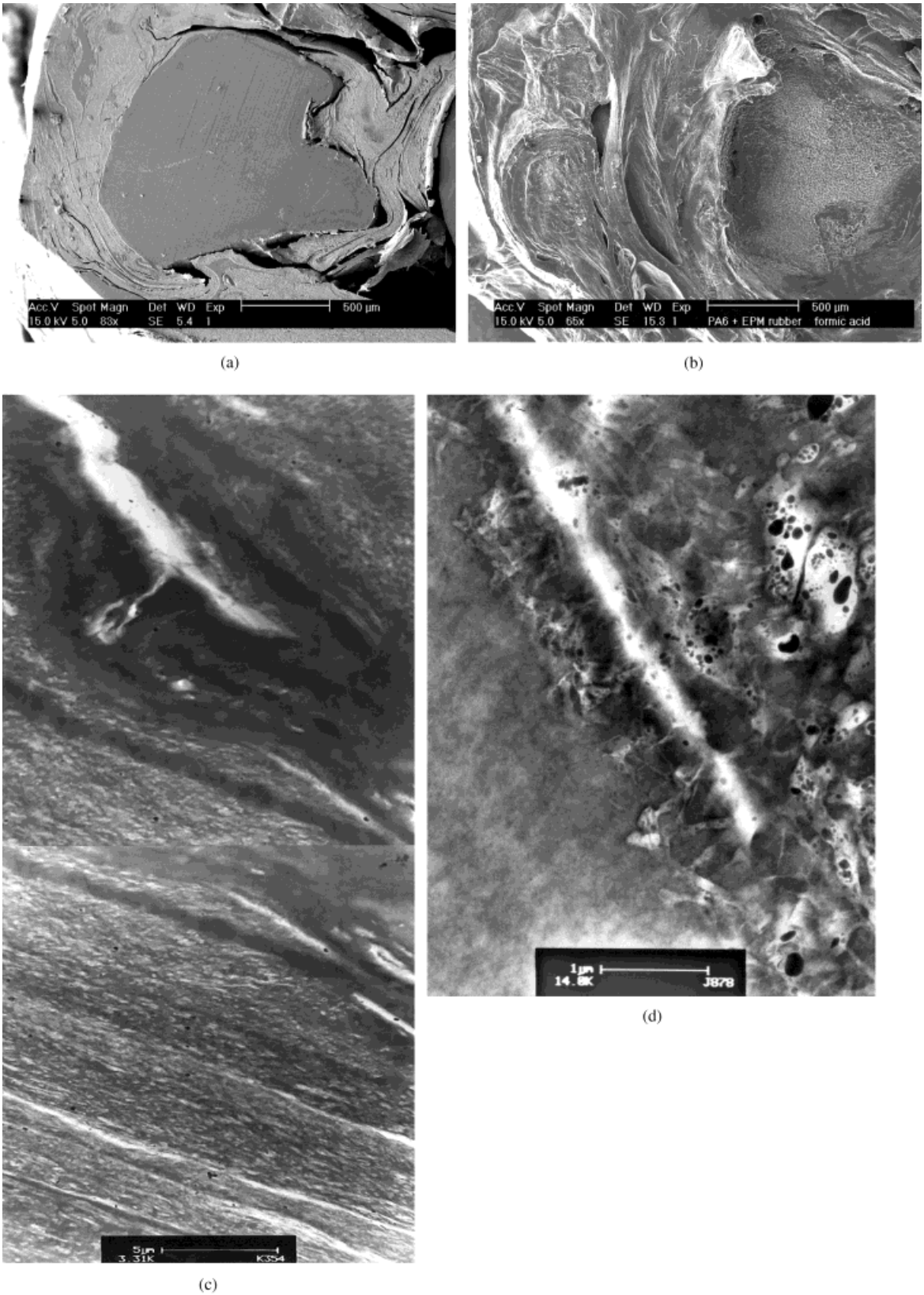

Figure 8 Micrographs of blend 12 [PA-6/EPM-*g*-MA (80/20 w/w)] collected at location C: (a) SEM of the sample, (b) SEM of the sample after dissolution of PA-6, (c) TEM panorama at the interface, and (d) TEM using higher magnification.

Table III PA-6 Occlusions in Dispersed EPM-*g*-MA Particles of PA-6/EPM-*g*-MA Blends as Function of Screw Length

Blend	Sampling Location	Fraction of Rubber Particles with PA-6 Occlusions
1	A	0.74
	B	0.86
	C	0.88
	D	0.85
10	A	0.20
	B	0.22
	C	0.18
11	C	0.70
	H	0.78
12	C	0.90
	H	0.88
13	C	0.73
	H	0.84

the interface, and there is no driving force for drawing these graft copolymer inside the rubber dispersion. This supports the assumption that occlusions are formed from PA-6/EPM-*g*-MA graft copolymers on the melting of PA-6 pellets.

In the blends with the other MA-containing polymers, no PA-6 occlusions were observed in the dispersed phase [Fig. 4(a–d)]. This may be attributed to the relatively high softening points of the other MA-containing polymers and/or to its high viscoelastic behavior.

CONCLUSIONS

Using sampling devices along the barrel of a twin-screw extruder allows a detailed study of chemical and morphological evolution during blending. It was shown that during melt blending of PA-6 and EPM-*g*-MA, both processes (chemical conversion and morphological development) are very fast, occurring within a few seconds over a few centimeters. Morphological evolution is associated with chemical conversion. When the MA groups of EPM-*g*-MA are almost completely converted, the morphology of the blend is also fully developed. However, by varying the experimental setup, it was possible to get a better insight into the process and obtain more information about morphological development. Replacing EPM-*g*-MA with MA-containing polymers that have higher softening temperatures and varying the processing conditions (particularly the temperature profile and the screw speed) affects the chemical conversion and therefores the morphological evolution.

The processing conditions used in this work (which are industrially relevant) along with the specific characteristics of the components used in the PA-6/EPM-*g*-MA blends produced final dispersion of rubber particles in the PA-6 matrix without phase inversion occurring.

Finally, it was shown that PA-6 the formation of occlusions in the dispersed rubber phase occurs during the melting and initial dispersion phase. The degree of occlusion is not affected by further processing.

The authors are grateful to DSM (Geleen, the Netherlands) for the materials and technical support; to Exxon (Barcelona, Spain) and to Eastman Kodak (Kingsport, TN) for materials; and to INVOTAN (Portugal) for financial support.

REFERENCES

1. Datta, S.; Lohse, D. Polymeric Compatibilizers; Hanser Publishers: New York, 1996.
2. Utracki, L. A. Encyclopaedic Dictionary of Commercial Polymer Blends; ChemTec Publishing: Toronto, 1994.
3. Datta, S.; Lohse, D. J. Polymeric Compatibilizers, Uses and Benefits in Polymer Blends; Hanser Publishers: Munich, 1996.
4. van Duin, M.; Aussems, M.; Borggreve, R. J. M. J Polym Sci, Part A: Polym Chem 1998, 36, 179.
5. Triacca, V. J.; Ziaee, S.; Barlow, J. W.; Keskkula, H.; Paul, D. R. Polymer 1991, 32, 1401.
6. Cartier, H.; Hu, G. H. J Polym Eng Sci 1999, 39, 996.
7. Mantia, F. P. Adv Polym Tech 1993, 12, 47.
8. Dali, S. S.; Xanthos, M.; Biesenberger, J. A. Polym Eng Sci 1994, 43, 1720.
9. Lee, J. D.; Yang, S. M.; Polym Eng Sci 1995, 35, 1821.
10. Ide, F.; Hasegawa, A. J Appl Polym Sci 1974, 18, 963.
11. Seadan, M.; Graebling, D.; Lambla, M. Polym Networks Blends 1993, 3, 115.
12. Lambla, M.; Seadan, M. Polym Eng Sci 1992, 32, 1587.
13. Huneault, M. A.; Champagne, M. F.; Luciani, A. Polym Eng Sci 1996, 36, 1694.
14. Stephan, M.; Franzheim, O.; Rische, T.; Heidemeyer, P.; Burkhardt, U.; Kiani, A. Adv Polym Tech 1997, 16, 1.
15. Sakai, T. Adv Polym Tech 1995, 14, 277.
16. Machado, A. V.; Covas, J. A.; van Duin, M. J Appl Polym Sci 1999, 71, 136.
17. Machado, A. V.; Covas, J. A.; van Duin, M. J Polym Sci, Part A: Polym Chem 1999, 37, 1311.
18. Sundararaj, U.; Macosko, C. W. Polym Eng Sci 1996, 36, 1769.
19. Scott, C. E.; Macosko, C. W. Polym Bulletin 1991, 26, 341.